Supporting Information

Ionic-Passivated FeS_2 Photocapacitors for Energy Conversion and Storage

Maogang Gong,[a] Alec Kirkeminde,[a] Nardeep Kumar,[b] Hui Zhao,[b] Shenqiang Ren[a,*]

a. Dr. M. Gong, A. KIekeminde, Prof. S. Ren.
Department of Chemistry
University of Kansas, Lawrence, KS 66045, USA
E-mail: shenqiang@ku.edu

b. N. Kumar, Prof. H. Zhao
Department of Physics
University of Kansas, Lawrence, KS 66045, USA

FeS_2 Nano crystals synthesis: The FeS_2 nanocrystals were prepared using a modified protocol from Puthussery et. al.[1] In detail, in one flask, 4 mmol sulfur solid particles was dissolved in 5 mL diphenyl ether and sonicated until all sulfur was dissolved and then degassed for one hour at 70 ^oC under argon. In a separate vessel 0.5 mmol of $FeCl_2$ is dissolved in 12 g Octadecylamine (ODA) and degassed for 1 hour at 120 ºC to allow for decomposition. For FeS_2 NS, the iron solution is then raised to 220 ^oC (for FeS_2 cubes the solution was kept at 120 ^oC) and the sulfur solution was rapidly injected into the iron solution. The solution immediately turned black upon injection. This solution was allowed to react for 90 min. After the reaction was finished, the solution was allowed to cool to ~100 ^oC and halted with injection of methanol and crashed out using the centrifugation. The FeS_2 nanocrystals were cleaned up using standard crash out/wash method using chloroform/methanol by the centrifugation in a N_2 glovebox. After cleaning the nanocrystals were redispersed in chloroform for storage and characterization.

Materials Characterization: All UV-Vis-NIR absorbance spectra were obtained on a UV-3600 Shimadzu Spectrophotometer. Room temperature x-ray powder patterns were obtained using monochromated Cu-Kα radiation (λ= 1.54178 Å) on a Bruker Proteum

Diffraction System equipped with Helios multilayer optics, an APEX II CCD detector and a Bruker MicroStar microfocus rotating anode x-ray source operating at 45 kV and 60 mA. The powders were mixed with a small amount of Paratone N oil to form a paste that was then placed in a small (< 0.5 mm.) nylon kryoloop and mounted on a goniometer head. Transmission Electron Microscope (TEM) images were obtained using Field Emission FEI Tecnai F20 XT. Field Emission Scanning Electron Microscope (FESEM) images were obtained using LEO 1550 FESEM.

Device Fabrication and Measurement: The photocapacitor devices are fabricated as following: The FeS_2 NS and cubes were dissolved in chloroform with concentration of 25 mg/mL and 40 mg/mL, respectively. The mixture of FeS_2 NS (25mg/mL) and cubes (40 mg/mL) is prepared with a volume ratio 2:1. The poly(3,4-ethylene dioxythiophene):poly(styrene sulfonate) (PEDOT:PSS) hole transport layer was spun-coated on the ITO substrate at 3000RPM for 1 min. The FeS_2 NS, FeS_2 cubes and mixture were deposited on the PEDOT:PSS/ITO surface by the spin-coating method at the speed of 1500 RPM for 1 min. The FeS_2 nanocrystals were originally capped with octadecylamine (ODA) surfactants, which were removed through an ethanedithiol (EDT) treatment in acetonitrile solvent. For the BMII-treated FeS_2 device, 20μL1-Butyl-3- methylimidazolium iodide (BMII) was dropped onto the FeS_2 nanocrystal surface, then spin coated at 3000RPM for 1min and drying on hot plat at 100^{o}C for 1 min. The process is similar as the [Hmim][Br], [Hmim][Tf_2N]-treated FeS_2 device. Finally, a patterned aluminum electrode (~80 nm) was evaporated on the top surface to complete the device.

The ionic liquid (IL) was allowed to seep into the porous FeS_2 active layer via spin coating and dried at 100^{o}C, which enabled the nanoparticles passivation by replacing long organic ligands and halide anion bonded to cations on nanoparticle surfaces.[2,3] To elaborate upon the particles capping process, there has been extensive work done on investigating how solution-cast materials infiltrate into mesoporous structures.[4-6] If the concentration of the

solution is low enough, and the solubility of the cast materials high enough, the materials will penetrate the pores as the solvent evaporates. Typically, the materials form a "wetting" layer upon the internal surface of the mesoporous film that uniformly coats the pore walls throughout the whole thickness of the active layer.[2,4] The degree of "pore-filling" can be controlled by varying the solution concentration.[5,6] If the concentration of the casting solution is high, then maximum pore filling occurs, and any "excess" materials form a "capping layer" on top of the filled mesoporous film surface. Since ILs does not evaporate quickly it allows better infiltration into pores in the active layer.

Figure S1 exhibit the cubic FeS_2 unit cell and the cross-sectional atomic force microscopy (AFM) image of FeS_2 device. It is important to note that pyrite's crystal structure is simple cubic much like NaCl and can be through of iron atoms occupying the sodium position and S_2^{-2} dumbells in place of the chlorine ion, which renders the Fe-dominant [100] surface. Figure S2 Shows the x-ray diffraction (XRD) of the as-synthesized, BMII and [Hmim][Br] passivated FeS_2 nanocrystals. The as-synthesized FeS_2 nanocrystals is consistent with the pyrite structure (JCPDS Card No 1-079-0617), without detectable marcasite, greigite, pyrrhotite, or other impurities. The most important information of the XRD results is that after passivation, the FeS_2 can keep its crystalline state and help minimize defect states.[2]

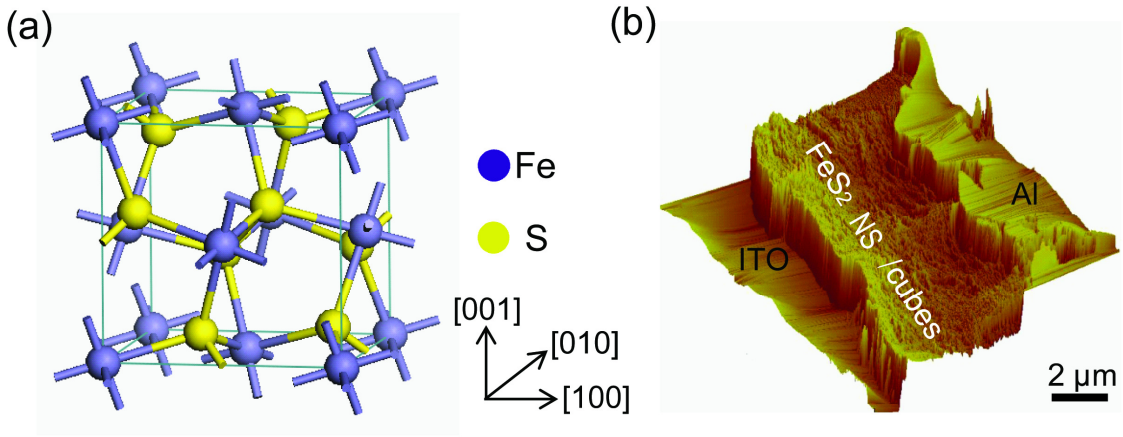

Figure S1: (a) The unit cell of FeS_2 structure. (b) The AFM cross-sectional image of FeS_2 NS/cube mixed device.

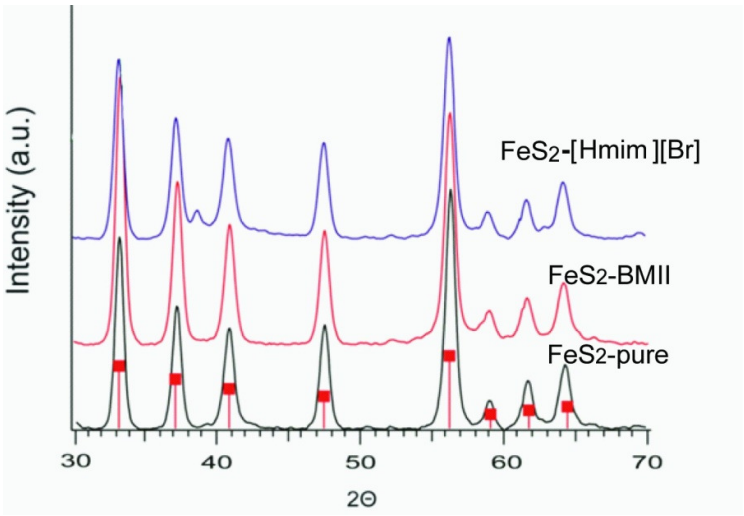

Figure S2: XRD spectrum of FeS_2 mixed crystal pure and coated by [Hmim][Br] and BMII, respectively.

Figure S3 show the TEM images of FeS_2 NS, cubes and mixture. The FeS_2 NS and cubes exhibit average 13.4nm diameter and a 47.5nm side length. The inset high resolution TEM image shows the lattice fringe of FeS_2 nanocrystals with the lattice spacing of 0.27nm, matching the (200) plane of pyrite. It can be seen in the mixture FeS_2 NS decorate very well around the bigger cubes. Figure S3 (d) shows the AFM side plan image of ITO/FeS_2 mixed/Al device.

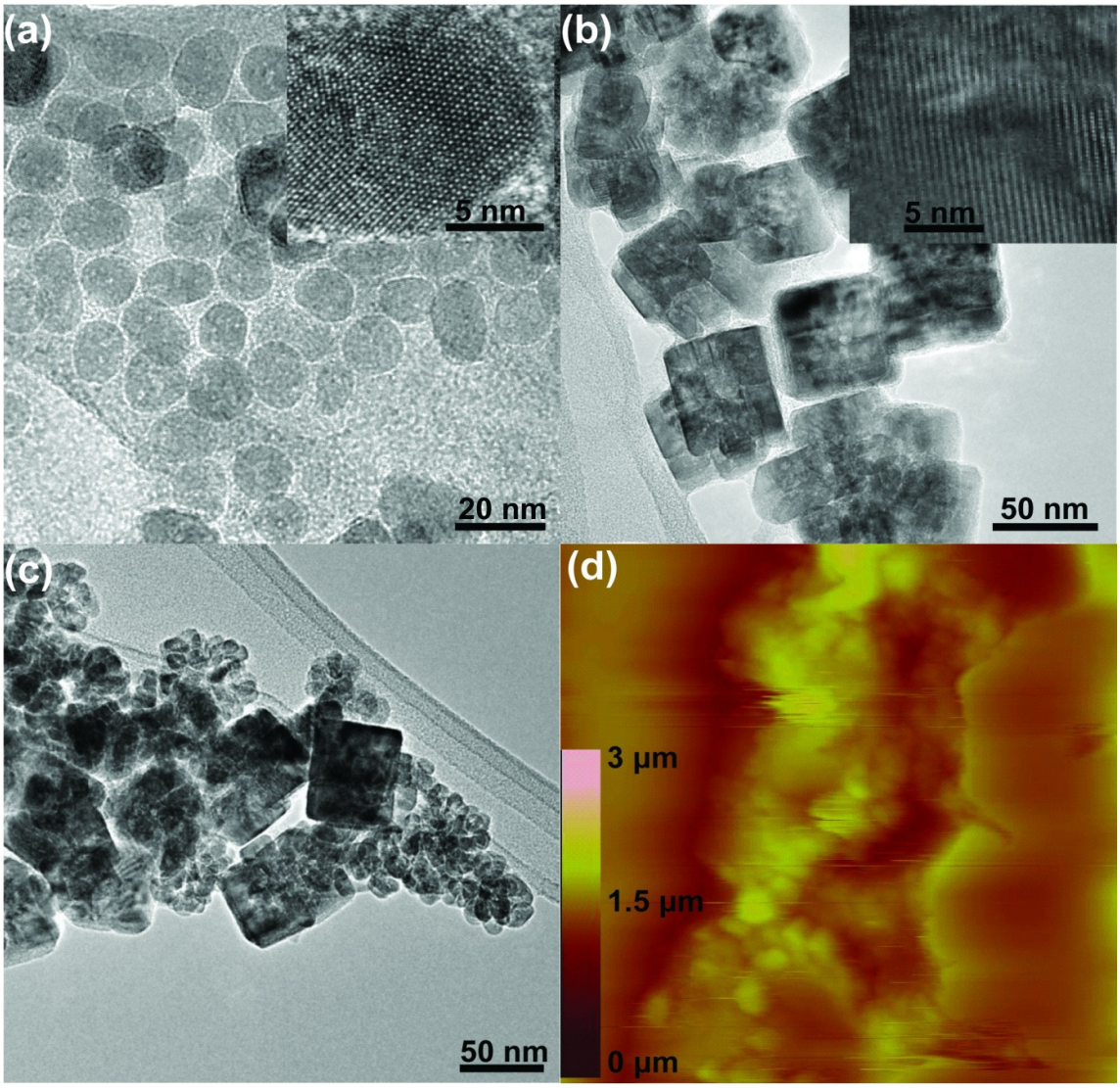

Figure S3: TEM images of FeS_2 NS (a), cubes (b) and mixture (c). AFM of the side plane of ITO/FeS_2 mixed/Al device is shown in image (d).

Figure S4 shows the carrier lifetime detected laser schematic set-up. A pump laser pulse of 100 fs and 750 nm injects charge carries by exciting electrons from the valence band to the conduction band. These carriers are probed by a time-delay probe pulse of 100 fs and 810 nm. Reflection of the probe is collected and sent to a photodiode, which output is measured by a lock-in amplifier. By modulating the intensity of the pump beam with a mechanical chopper, we can measure the differential reflection, defined as $\Delta R/R_o=(R-R_o)/R_o$, where R and Ro are the reflections with and without the presence of the pump, respectively.

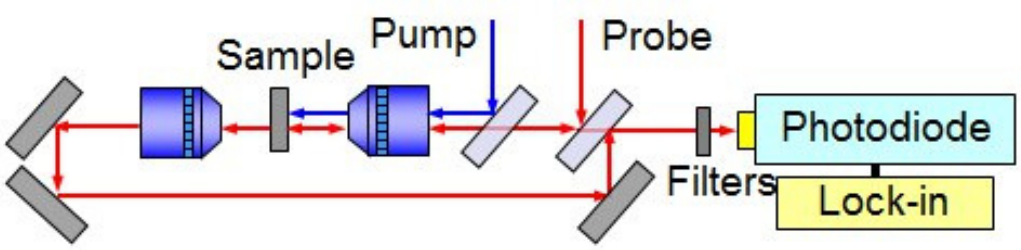

Figure S4: Schematic setup of the carrier lifetime detector instrumentation.

To examine the exchange of ODA by the halide anions, the pyrite particles were immersed into the BMII and then washed with methanol following protocol from literature,[2] in which I^- will bind to the iron-rich surface of the pyrite particles. Fourier transform infrared spectroscopy (FTIR) spectra (Figure S5) show the complete removal of the octadecylamine ligands (-CH_3 vibrations at 2874 cm^{-1} and 2959cm^{-1}, -CH_2 vibration1462cm^{-1} and 2935cm^{-1}, and –NH_2 vibration 3082cm^{-1} and 3144cm^{-1}).

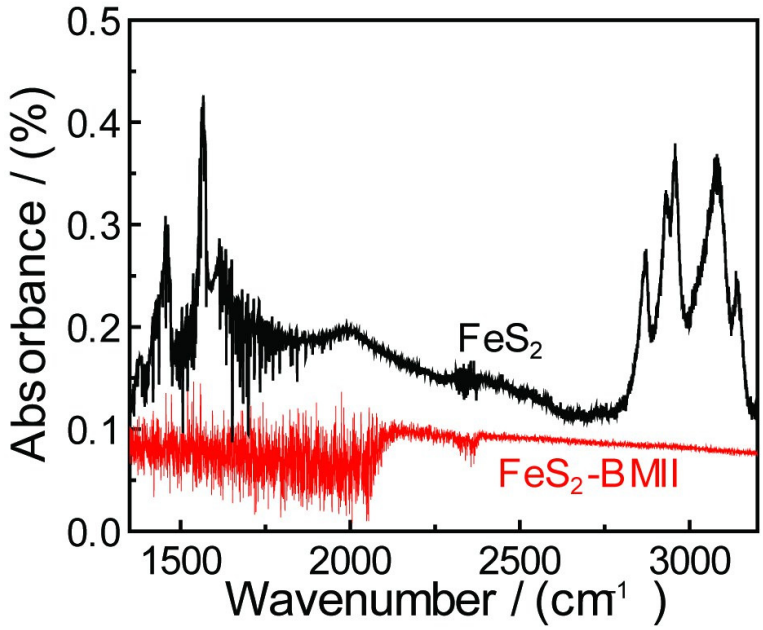

Figure S5. FTIR absorption spectrum of pure FeS_2 NS-cubs mixed and BMII modified FeS_2 NS-cubs mixed nanocrystals.

Figure S6 (a) gives the comparison of photocurrent among the FeS_2 NS, cube, and mixture based devices with EDT ligand exchange utilized. Cube-only pyrite active material exhibits the lowest photocurrent. When replacing cubes with NS, the photocurrent increases

significantly. By mixing the FeS_2 NS and cube together, the photocurrent reaches its maximum. It has been shown that cubes are more active than the quantum dots, but require a matrix surrounding them to help with charge transport due to their large size and poor stacking in films. Knowing that the mixture of both shapes gives the best performance, different ILs are tested to compare the effect of different halide ions on the photocurrent generation. It can be seen in Fig. S6 (b) that a higher photocurrent is observed by using the [Hmim][Br] than that of the EDT based passivation. When replacing the Br^- ion with the I^- ion in the BMII ionic liquid, the current again takes an even more substantial enhancement. The increase in the photocurrent could be related to the passivation of the pyrite surface defects, where the I^- ions show better effective passivation than that of Br^-, matching with previous results.[7]

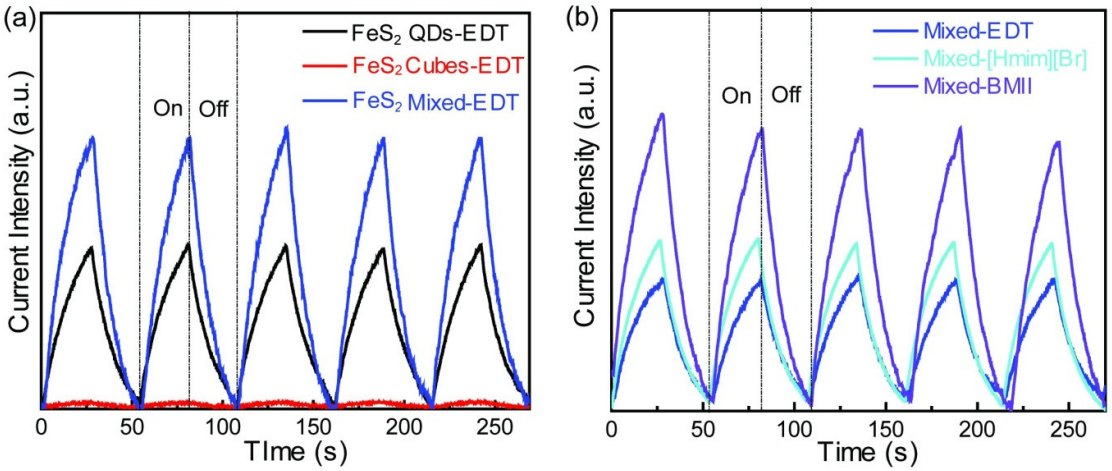

Figure S6: (a) The comparison of photocurrent among the FeS_2 NS, cube, and mixture based devices with EDT ligand exchange utilized. (b) Different halide ions effect on the photocurrent.

The photoresponsivity and detectivity of FeS_2 photocapacitor under the 1100 nm NIR illumination is shown in Fig. S7a. Figure S7b shows cyclic voltammetry (CV) curves of BMII modified ITO/PEDOT:PSS/FeS_2/Al photocapacitor device under different sweep rates of 0.1,

0.2, 0.3, 0.4 and 0.5V/s. The CV curves remained similar shapes for the different scan rates, indicating a high electrochemical stability and capacitance.

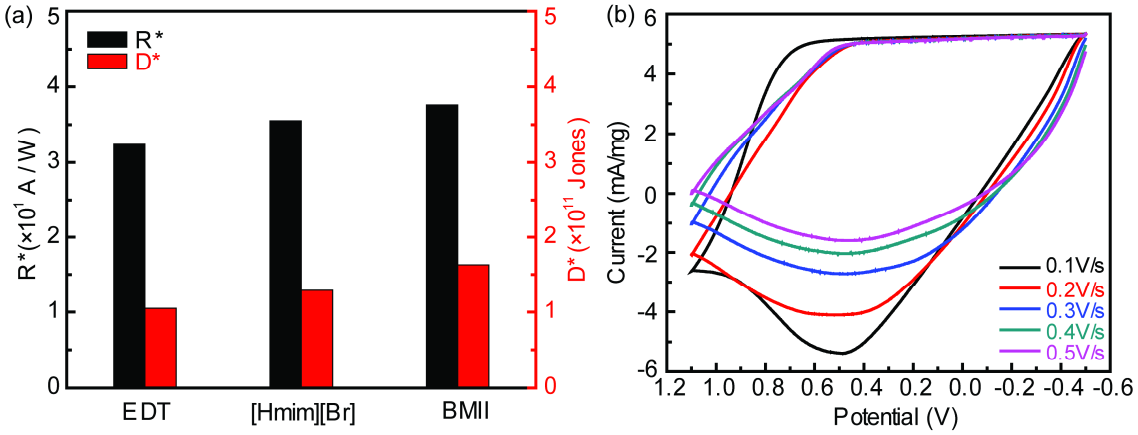

Figure S7: (a) The photoresponsivity and detectivity of FeS_2 photocapacitor under the 1100 nm NIR illumination. (b) Cyclic voltammograms based on BMII passivated hybrid FeS_2 device ITO/PEDOT:PSS/FeS_2/Al with different sweep rates of 0.1, 0.2, 0.3, 0.4 and 0.5 V/s.

Figure S8 (left image) shows the current-time (I-t) characteristics of the FeS_2 photocapacitor modified with [BMII] and [Hmim][Tf_2N], respectively. Figure S8 (right image) shows the FeS_2 hybrid photocapacitor charge-discharge voltage-time (V-t) characteristics. It can be seen that changing the anion has a significant impact on the photoinduced voltage. This can be attributed to the I^- passivation of pyrite, which creates an improved double layer. Discharging voltage of the photocapacitor is seen to be much faster by utilizing the I^- ion, which can be ascribed to the smaller anion size resulting in quicker movement.

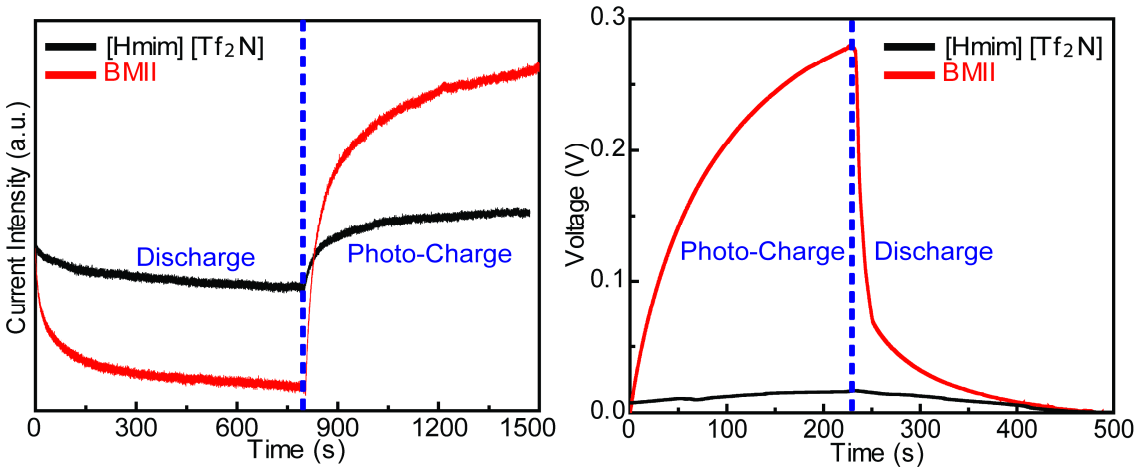

Figure S8: The current-time (I-t) characteristics of FeS_2 photocapacitor modified with [BMII] (red line) and [Hmim][Tf_2N] (black line), left image. The charge-discharge V-t characteristics of FeS_2 hybrid photocapacitor, modified by the BMII and [Hmim][Tf_2N], right image.

References

1 J. Puthussery, S. Seefeld, N. Berry, M. Gibbs and M. Law, *Journal of the American Chemical Society*, 2010, **133**, 716.

2 J. Tang, K. W. Kemp, S. Hoogland, K. S. Jeong, H. Liu, L. Levina, M. Furukawa, X. Wang, R. Debnath, D. Cha, K. W. Chou, A. Fischer, A. Amassian, J. B. Asbury and E. H. Sargent, *Nat Mater.*, 2011, **10**, 765.

3 D. Zhitomirsky, M. Furukawa, J. Tang, P. Stadler, S. Hoogland, O. Voznyy, H. Liu and E. H. Sargent, *Advanced Materials*, 2012, **24**, 6181.

4 (a) M. M. Lee, J. l. Teuscher, T. Miyasaka, T. N. Murakami and H. J. Snaith, *Science*, 2012, **338**,643; (b) T. Leijtens, I. K. Ding, T. Giovenzana, J. T. Bloking, M. D. McGehee and A. Sellinger, *ACS Nano*, 2012, **6**, 1455.

5 (a) J. Melas-Kyriazi, I. K. Ding, A. Marchioro, A. Punzi, B. E. Hardin, G. F. Burkhard, N. Tétreault, M. Grätzel, J.-E. Moser and M. D. McGehee, *Advanced Energy Materials*, 2011, **1**, 407; (b) I. K. Ding, N. Tétreault, J. Brillet, B. E. Hardin, E. H. Smith, S. J. Rosenthal, F. Sauvage, M. Grätzel and M. D. McGehee, *Advanced Functional Materials*, 2009, 19, 2431.

6 P. Docampo, A. Hey, S. Guldin, R. Gunning, U. Steiner and H. J. Snaith, *Advanced Functional Materials*, 2012, **22**, 5010.

7 A. Ennaoui, S. Fiechter, C. Pettenkofer, N. Alonsovante, K. Buker, M. Bronold, C. Hopfner and H. Tributsch, *Sol. Energy Mater. Sol. Cells*, 1993, **29**, 289.